ELSEVIER

Polymer 42 (2001) 4501–4507

polymer

www.elsevier.nl/locate/polymer

Synthesis and thermal behaviour of layered silicate–EVA nanocomposites

M. Zanetti[a], G. Camino[a,*], R. Thomann[b], R. Mülhaupt[b]

[a]*Dipartimento do Chimica Inorganica, Chimica Fisica e Chimica del Materiali dell'Universita, Università degli Studi di Torino, IFM Via P. Giuria 7, 10125 Torino, Italy*

[b]*Freiburger Materialforschungszentrum und Institut für Makromolekulare Chemie der Albert-Ludwigs Universität, Stefan-Meier-Str. 31, D-79104 Freiburg i. Br., Germany*

Received 20 August 2000; received in revised form 17 October 2000; accepted 22 October 2000

Abstract

Extrusion moulding of both polymer-layered silicate nanocomposites and microcomposites based on the copolymer poly (ethylene-*co*-vinylacetate) with either 12 wt.% (EVA 12) or 19 wt.% (EVA 19) vinyl acetate content is described in this paper. The silicates were a synthetic fluorohectorite, rendered organophilic by means of cation exchange of intergallery sodium cations for octadecylammonium or ammoniumdododecanoic acid, and a montmorillonite, rendered organophilic with octadecylammonium. The materials thus obtained were characterised by wide angle X-ray diffraction and transmission electron microscopy. It was established that dispersion of the organic phase depends on both the silicate type and silicate modification. At these vinylacetate contents dispersion was achieved without requiring additional compatibiliser. The thermal behaviour of the composites was examined on a thermobalance in nitrogen and in air. In the nanocomposites acceleration of EVA deacylation and slower thermal degradation were observed, while protection against thermo-oxidation and delayed weight loss were evident in air.

Keywords: Thermal behaviour; Layered nanocomposites; Extrusion moulding

1. Introduction

Polymers are filled with an inorganic component to increase their strength or impact resistance, to reduce their electrical conductivity and permeability of oxygen and other gases [1]. These improvements increase as a function of the length/diameter ratio (aspect ratio) and dispersion of the inorganic phase and are limited in conventional filled polymers by the distinct macroscopic separation of the two phases.

This restriction is overcome in a new class of materials known as polymer-layered silicate nanocomposites (PLSN) because the particles in their dispersed phase are of the order of a few nanometers [2–5]. The layered silicates used for this purpose are mica, fluoromica, montmorillonite, vermiculite, hectorite, fluorohectorite, saponite, etc. [6,7] and belong to the structural family known as the 2:1 phyllosilicates. Their crystalline structure consists of a two-dimensional lamina obtained by blending two tetrahedral silica layer with metal atoms (i.e. Mg for talc and Al for mica) to form a corresponding octahedral metal oxide layer. The lamina thickness is around 1 nm while the lateral dimensions range from 0.5 to several microns. Each lamina is separated from the next by a van der Waals gap called gallery or interlayer. These galleries are normally occupied by cations that counterbalance the excess negative charge generated by the isomorphous substitution of the atoms forming the crystal (i.e. Mg^{2+} or Fe^{2+} replacing Al^{3+} in montmorillonite and Li^{+} replacing Mg^{2+} in hectorite), and are usually alkaline and hydrated alkaline-earth metal cations. Dispersion of the silicate particles in the polymer matrix is improved by replacing these metal cations with ions bearing an aliphatic chain so as to compatibilise the silicate and enhance its interaction with the polymer by enlarging the interlayers. These silicates are usually known as organoclays.

Interactions between macromolecules and layered silicates have been studied for many years [8]. Their practical exploitation began with the production of a nanocomposite nylon developed by Okada et al. [9,10] in Toyota's laboratories.

Direct dispersion of the organoclay in the molten

* Corresponding author. Tel.: +390-11-670-7557; fax: +390-11-670-7855.
E-mail address: camino@silver.ch.unito.it (G. Camino).

0032-3861/01/$ - see front matter
PII: S0032-3861(00)00775-8

Table 1
The materials

Abbreviation	Polymer	Silicate	Type
EVA12-*or*-EVA19	Poly(ethylene-*co*-vinylacetate)	None	Pure polymer
EVA12(19)–FH/ODA	Poly(ethylene-*co*-vinylacetate)	Fluorohectorite exchanged with octadecylammonium	Nanocomposite
EVA12(19)–FH/ADA	Poly(ethylene-*co*-vinylacetate)	Fluorohectorite exchanged with aminodedecanoic acid	Microcomposite
EVA12(19)–MMT/ODA	Poly(ethylene-*co*-vinylacetate)	Montmorillonite exchanged with octadecylammonium	Mixed nanocomposite

polymer with an extruder is the most appropriate technique for the industrial preparation of PLSN. Two classes are obtained: intercalated nanocomposites, where the polymer chains are intercalated in the galleries, and delaminated or exfoliated nanocomposites, where the delaminated silicate is uniformly dispersed in the matrix. The aspect ratio and the dispersion attain very high values in delaminated nanocomposites. Lamellae aspect ratio ranging from 100 to 1000 result in polymers with high rigidity and heat stability, reduced gas permeability and good transparency with as little as 5–10 wt.% silicate. Recent combustion data have shown that PLSN may be suitable for the elaboration of new flame retardant polymer material [11–13].

This paper describes the thermal properties of nanocomposites formed from poly(ethylene-*co*-vinyl acetate) (EVA). The inorganic phase was fluorohectorite or montmorillonite, both exchanged with octadecyl ammonium. The results obtained with a microcomposite based upon EVA filled with fluorohectorite exchanged with aminodedecanoic acid are also shown for comparison.

2. Experimental

2.1. Materials

The copolymers used were EVA with 12 and 19 wt.% vinyl acetate (Exxon's Escorene UL0012 and UL0019): EVA 12 and EVA 19, respectively.

The fluorohectorite-like synthetic silicate Somasif (TM) ME 100 (FH) was supplied by Co-Op Ltd, Japan. The negative charges of its layers were compensated with Na^+ ions. The cation exchange capacity was between 0.7 and 0.8 meq/g. X-ray diffraction (XRD) showed that the spacing of the interlayer was 0.95 nm. The cation exchange was carried out with two swelling agents: octadecylammonium (ODA) and aminodedecanoic acid (ADA) as already described [14]. The montmorillonite exchanged with ODA (MMT/ODA) was supplied by Süd-Chemie.

2.2. Compounding

The materials studied were obtained by mixing EVA12 and EVA19 with organoclays at 120°C for 5 and 10 min in a DACA twin-screw minicompounder. The same procedure was used to prepare the pure EVA controls. The characteristics and names of the four materials are illustrated in Table 1.

2.3. Characterisation

Ultrathin sections of the composites with a thickness of approximately 50 nm were prepared with an ultra microtome (Ultracut e., Reichert and Jung) equipped with a diamond knife. Transmission electron microscopy (TEM) was carried out with a Zeiss TEM 912 using an accelerator voltage of 120 keV. Due to the high electron density differences between silicate and polymer, staining of the samples was not necessary.

The thickness of the interlayer was measured by XRD. The composites were analysed in film while the organoclays in powder. A Philips diffractometer was used with CoK_α radiation ($\lambda = 0.179$ nm).

Thermodegradation was determined on approx. 10 mg samples in a TGA 2950 balance (TA Inc.) with alumina sample pan in a 60 cm^3/min nitrogen flow and with a 10°C/min heating ramp.

Thermo-oxidation was determined in the same way in a 60 cm^3/min air flow.

3. Results and discussion

3.1. Morphology

FH is a hectorite obtained by heating talc in the presence of Na_2SiF_6. It was rendered organophilic by exchanging the intergallery sodium cations for protonated ODA to form FH/ODA and with protonated ADA to form FH/ADA. Formation of a nanocomposite from this silicate depends on the type of silicate modification employed. Our results show that exfoliation can be achieved at least at vinylacetate

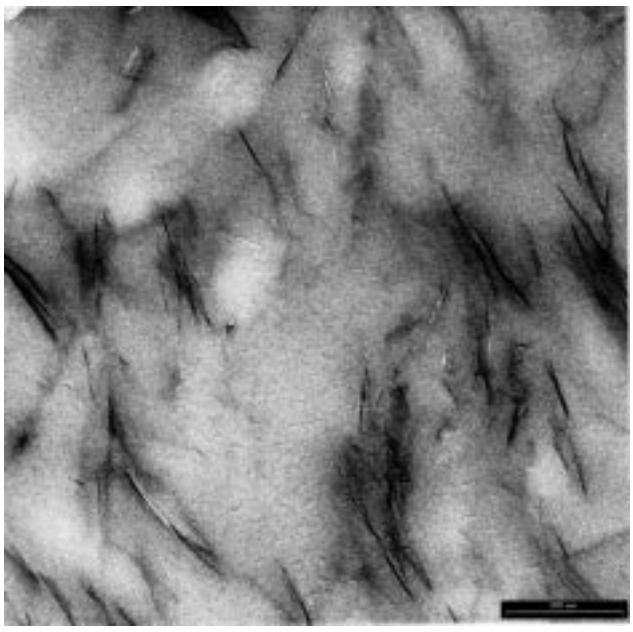

Fig. 1. TEM images of nanocomposites based upon EVA19 filled with 5 wt.% synthetic fluorohectorite exchanged with octadecylammonium (EVA19–FH/ODA).

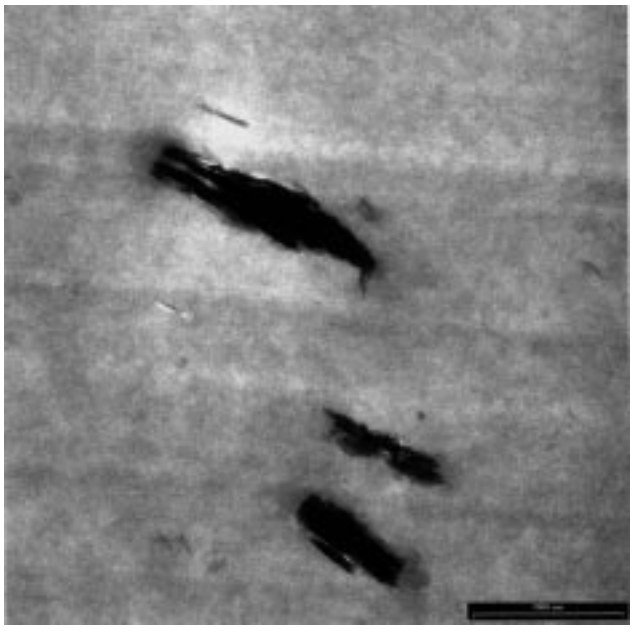

Fig. 3. TEM images of microcomposite based upon EVA19 filled with 5 wt.% synthetic fluorohectorite exchanged with ammoniumdodecanoic acid (EVA19–FH/ADA).

content ≤12%, without requiring additional matrix compatibilisation.

3.2. Nanocomposite

Fig. 2 shows a comparison of both XRD traces of FH/ODA and EVA19–FH/ODAQ. The *d*001 peak at 5.2 2θ corresponds to a 2 nm interlayer spacing, while the flat trace for the composite sample shows that the silicate laminae have lost their reciprocal order at a distance smaller than 501 nm. The TEM image of EVA19–FH/ODA is reported in Fig. 1, exhibiting the very effective exfoliation of the silicate to form a delaminated nanocomposite.

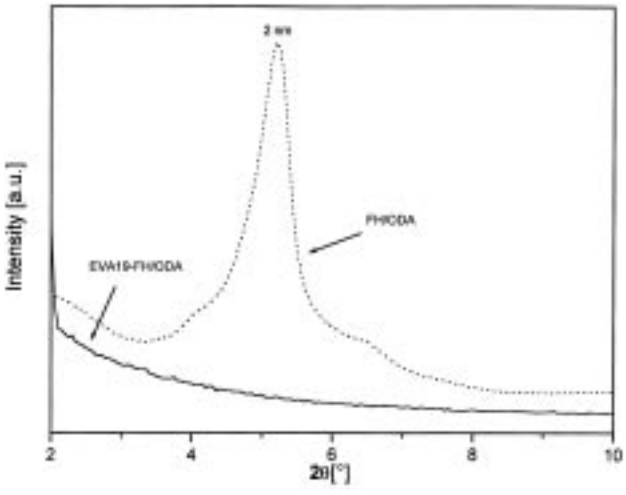

Fig. 2. X-ray diffraction pattern of fluorohectorite exchanged with octadecylammonium (FH/ODA) compared with XRD pattern of the nanocomposite obtained from the melt extrusion of EVA19 with 10 wt.% of fluorohectorite exchanged with ottadecylammonium (EVA19–FH/ODA).

3.3. Microcomposite

Using ADA for silicate modification, the compatibility of organoclay and polymer was poor and insufficient to afford nanocomposite formation. In the TEM image of EVA19–FH/ADA (Fig. 3) the primary particles, composed of many silicate layers, can be seen. The similarly peaked curves for FH/ADA and EVA19–FH/ADA in Fig. 4 show that there is

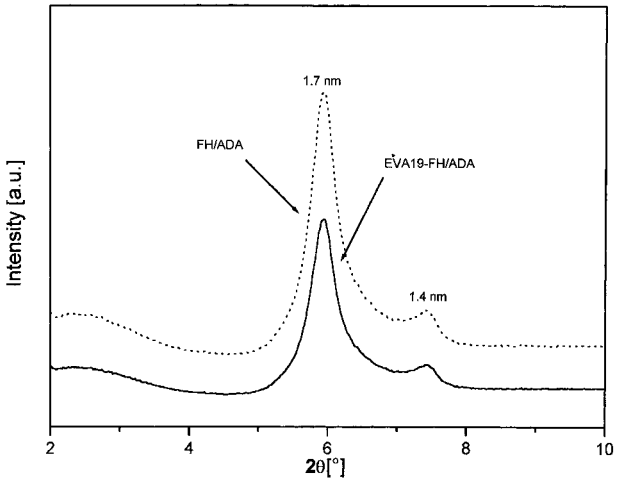

Fig. 4. XRD pattern of fluorohectorite exchanged with ammoniumdodecanoic acid (FH/ADA) compared with that of the microcomposite obtained from the melt extrusion of EVA19 with 10 wt.% of fluorohectorite exchanged with ammoniumdodecanoic acid (EVA19–FH/ADA).

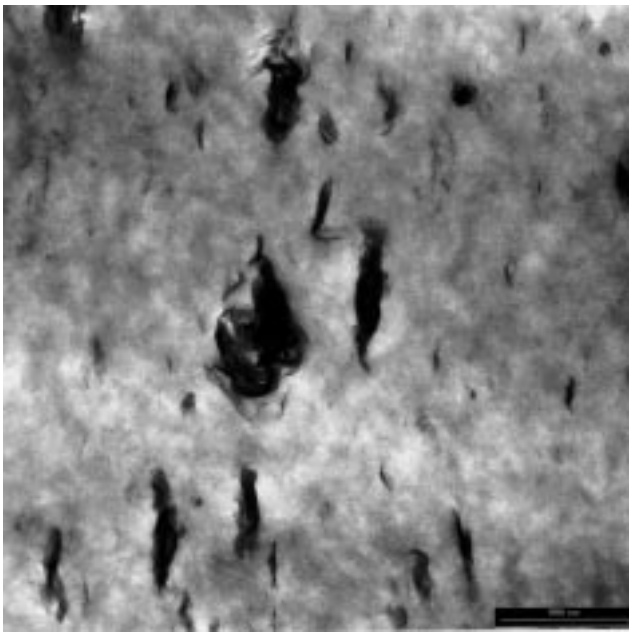

Fig. 5. TEM images of nanocomposites based upon EVA19 filled with 5 wt.% montmorillonite exchanged with octadecylammonium (EVA19–MMT/ODA).

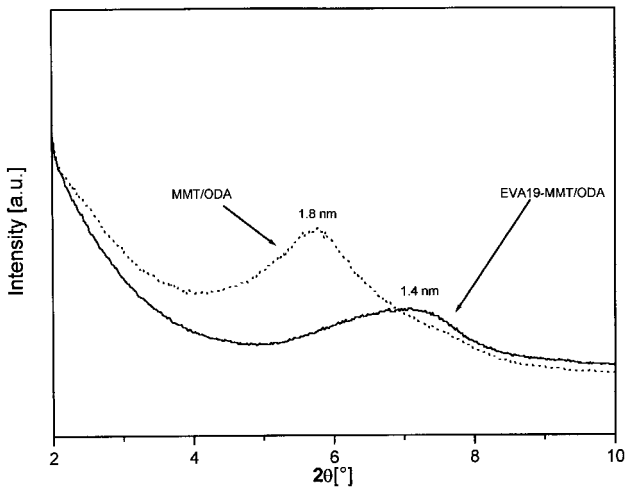

Fig. 6. XRD pattern of montmorillonite exchanged with octadecylammonium (MMT/ODA) compared with that of the nanocomposite obtained from the melt extrusion of EVA19 with 10 wt.% of montmorillonite exchanged with octadecylammonium (EVA19–MMT/ODA).

not intercalation of the polymer between the layers. This situation corresponds to that of a conventional filled polymer were, at least, each primary particle is dispersed in the polymer matrix.

3.4. Mixed nanocomposite

A different behaviour is displayed by MMT/ODA. The TEM picture of EVA–MMT/ODA (Fig. 5) shows a more complex situation with respect to the previously described composites. Here the organoclay (MMT/ODA) is not dispersed in a regular manner. Fig. 5 exhibits single exfoliated lamellae, tactoids composed of a variable number of lamellae and aggregates of tactoids. However the XRD analysis proves the formation of an intercalation hybrid. Combination with EVA19, in fact, results in the disappearance of the 1.8 nm interlayer peak and the appearance of a smoother peak corresponding to 1.4 nm at a higher 2θ angle (Fig. 6). This could be due to non-modified MMT present in the commercial product as an impurity and revealed by intercalation with ODA, or to partial thermal decomposition and volatilisation of ODA [15] during the extrusion (Scheme 1) followed by collapse of the interlayer. XRD, however, does not rule out intercalation at a distance greater than the 5.1 nm that would not be detectable by the instrument. If this were so, the exfoliated silicate would be flanked by areas with microscopic silicate dispersion. Results comparable to EVA19 were obtained with EVA12 compounded with the three organoclays.

3.5. Thermodegradation

Thermodegradation of EVA takes place in two stages. In the first, deacylation with the elimination of acetic acid and the formation of double bonds occurs between 300 and 400°C with a maximum around 350°C (Fig. 7). Radical and an ionic beta-elimination mechanisms (Scheme 2) have been proposed for this reaction [16,17].

Fig. 7 illustrates the effect of the nanocomposite on this stage. EVA19–FH/ADA, where the silicate is dispersed microscopically, behaves in the same way as EVA19, whereas deacylation is greatly accelerated in the exfoliated EVA19–FH/ODA. Here, in fact, the temperature range is 250–300°C with the maximum at about 280°C. The intensity, too, is one order of magnitude greater than that of EVA19. This acceleration is likely to be due to acid catalysis of the elimination reaction by protonated silicate formed from 200°C owing to the decomposition of ODA [18] (Scheme 3). The deacylation pattern of EVA19–MMT/ODA lies between those of EVA19 and EVA19–FH/ODA and consists of two partly overlapping stages. The first starts at 280°C, as for EVA19–FH/ODA, but proceeds more slowly to a maximum at about 285°C compared with 280°C for EVA19–FH/ODA and about 350°C for EVA19, the second is similar to that for

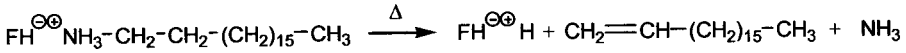

Scheme 1.

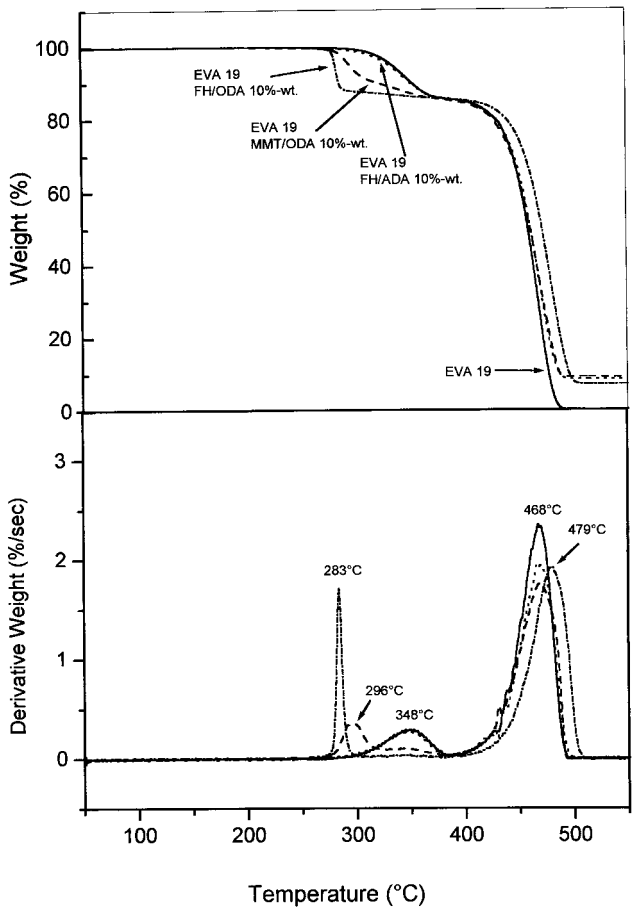

Fig. 7. TG curves in nitrogen on heating ramp of 10°C/min of: the nanocomposite of EVA19 with 10 wt.% of fluorohectorite exchanged with octadecylammonium (EVA19–FH/ODA), the microcomposite EVA19 with 10 wt.% of fluorohectorite exchanged with ammoniumdodecanoic acid (EVA19–FH/ADA), the mixed nanocomposite of EVA19 with 10 wt.% of montmorillonite exchanged with octadecylammonium (EVA19–MMT/ODA) and the pure EVA19.

EVA19. Indirect, but clear evidence is thus provided of the state of dispersion of the silicate in the EVA.

At temperatures higher than 380°C, thermal degradation of the ethylene-*co*-acetylene random copolymer resulting from deacylation takes place. The weight loss curves are much the same for EVA19, EVA19–MMT/ODA and EVA19–FH/ADA, whereas EVA19–FH/ODA displays a slight stabilisation of about 10°C throughout the process (Fig. 7). The patterns for the EVA12 and EVA19 materials are virtually identical apart from the lower deacylation weight loss when less vinyl acetate is present. The residue always consisted of the layered silicate.

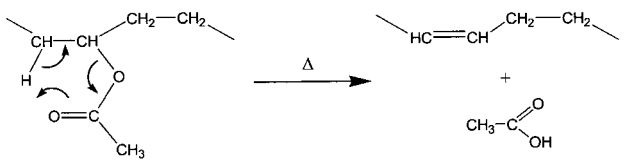

Scheme 2.

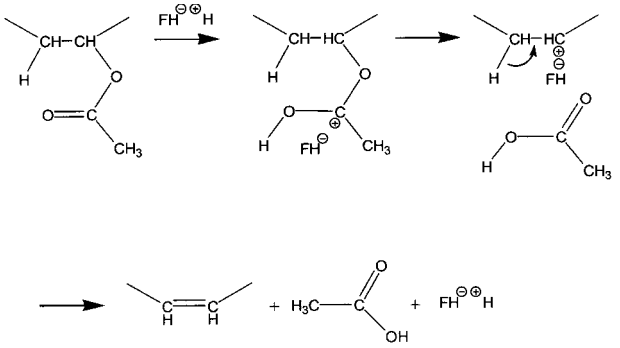

Scheme 3.

3.6. Thermo-oxidation

Comparison of the TG curves for EVA19 in nitrogen and air (Fig. 8) shows that air destabilises the polymer and speeds up both deacylation (maximum from 350 to 338°C) and degradation (maximum from 470 to 425°C). The polymer forms a 5% residue at 430°C, which is completely oxidised to volatile products between 470 and 550°C.

As can be seen in Fig. 9, EVA19–FH/ODA displays a different pattern. The presence of 5 wt.% exfoliated FH/ODA is enough to change the polymer's thermo-oxidation behaviour. The weight loss stage due to deacylation displays two rate maxima, one similar to that observed for EVA19–FH/ODA, under nitrogen, at about 283°C in Fig. 7, the other (barely visible in Fig. 9) at about 350°C, as for EVA19. The

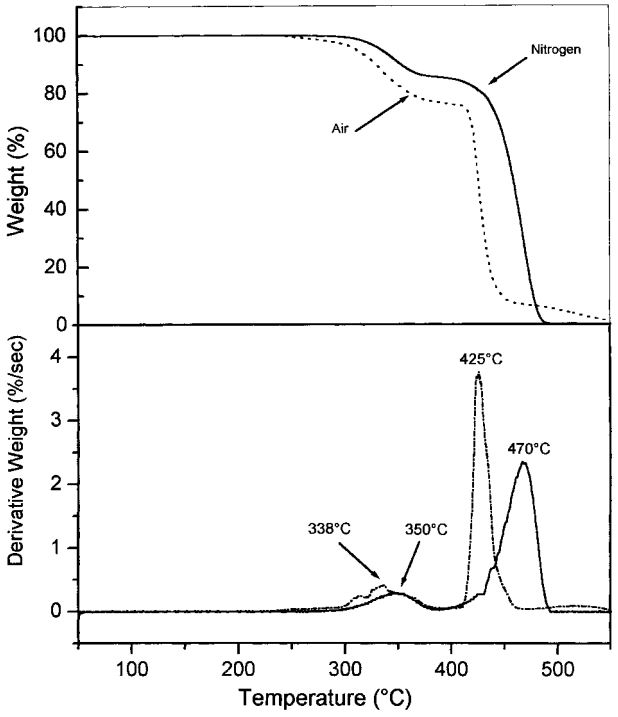

Fig. 8. TG curves in nitrogen and air on heating ramp of 10°C/min of pure EVA19.

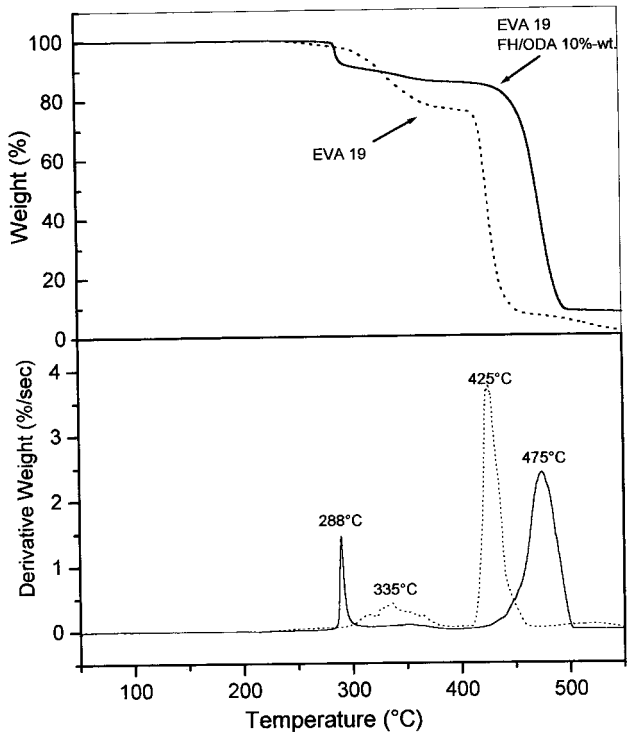

Fig. 9. TG curves in air on heating ramp of 10°C/min of: the nanocomposite of EVA19 with 5 wt.% of fluorohectorite exchanged with ottadecylammonium (EVA19–FH/ODA) and the pure EVA19.

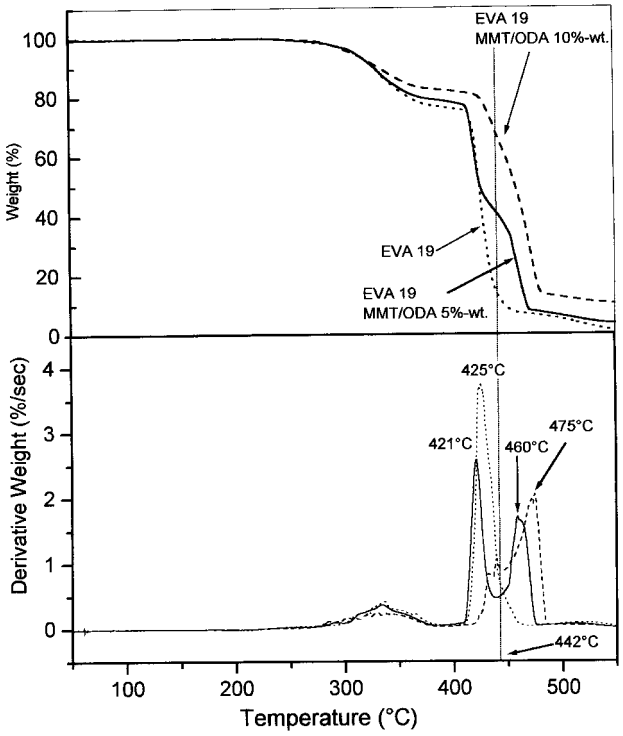

Fig. 10. TG curves in air on heating ramp of 10°C/min of the nanocomposites of EVA19 with 5 and 10 wt.% of montmorillonite exchanged with octadecylammonium (EVA19–MMT/ODA) compared with the pure EVA19.

TG curve (not shown) for EVA19–FH/ODA with 10 wt.% FH/ODA and thus with a greater polymer/silicate contact surface displayed a single peak at 283°C, in keeping with the view that deacylation is determined by a catalytic effect of the silicate layers. At temperatures higher than 400°C, degradation of EVA19–FH/ODA passes through a weight loss stage with a rate maximum at 473°C as in nitrogen. EVA19–FH/ODA thus behaves in much the same way in air and nitrogen. The exfoliated silicate completely shields the polymer from the action of oxygen.

The TG curves for EVA19 and 5 or 10 wt.% EVA19–MMT/ODA in air are compared in Fig. 10. EVA19–MMT/ODA don't show the catalysis of deacylation found for the 10% form in nitrogen (Fig. 7). Even so, 10% MMT/ODA protects against thermo-oxidation in much the same way as 5 wt.% FH/ODA because it gives most of the volatilisation with a rate maximum at a temperature (475°, Fig. 10) similar to that of 5 wt.% EVA19–FH/ODA (473°C, Fig. 9). The TG curve for 5 wt.% EVA19–MMT/ODA displays two stages of thermal volatilisation, one with a maximum at 421°C, typical for EVA19, the other with a maximum at 460°C, i.e. between 425°C for EVA19 and 473°C for 5 wt.% EVA19–FH/ODA (Fig. 9). The weight loss is about 35 wt.% in both stages. Absence of protection on the part of the silicate in the first stage is indicated by the similarity of the initial segments of the EVA19 and 5 wt.% EVA19–MMT/ODA curves. EVA19–FH/ADA behaves in air in the same way as EVA19.

In contrast to thermal degradation, where only the type of silicate and the type of silicate modifier are influential, the TG curves for the EVA12 materials (Fig. 11) show that thermo-oxidation is also dependent on the vinyl acetate content. The deacylation patterns for EVA12–FH/ADA and EVA12–MMT/ODA are similar and their weight loss is less than that of EVA12. Weight loss is also delayed for the two composites as compared to EVA12 in the second decomposition stage with a larger delay for EVA12–MMT/ODA probably due to its nanoscopic dispersed silicate fraction. The behaviour of the organoclay FH/ADA in EVA12 is thus different from EVA19 where it did not modify the thermal decomposition of the pure EVA19.

The effects are more evident in EVA12–FH/ODA, where the silicate is exfoliated and well dispersed. The usual acceleration of deacylation around 300°C is evident in the curve. Deacylation of EVA19, however, is not only accelerated but also begins at lower temperature (290°C, Fig. 9) as compared to that of both EVA12 and EVA12–FH/ODA beginning at 300°C (Fig. 11). Further thermal degradation of the deacylated polymer is the same as that of the pure polymer in nitrogen. Effective oxygen shielding is apparently provided.

4. Conclusions

This study has demonstrated that creation of nanocomposites by extrusion of EVA depends on both the type

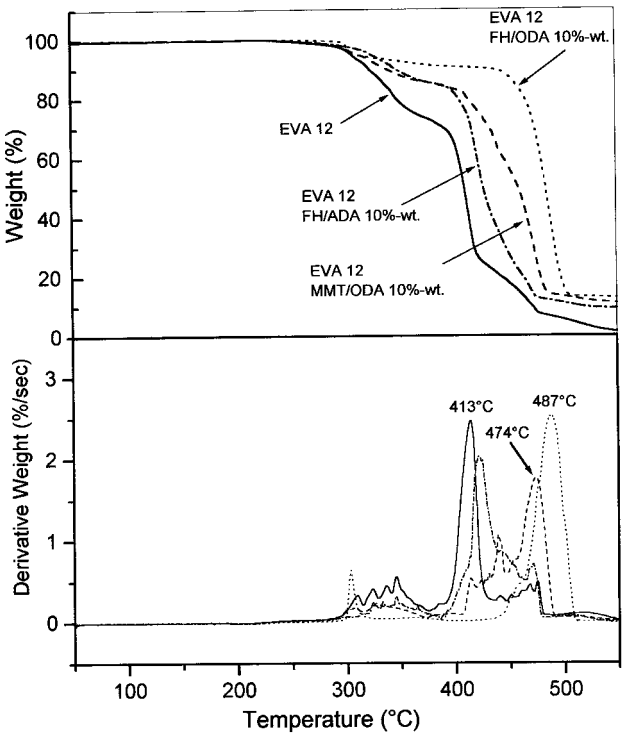

Fig. 11. TG curves in air on heating ramp of 10°C/min of: the nanocomposite of EVA12 with 10 wt.% of fluorohectorite exchanged with octadecylammonium (EVA12–FH/ODA), the microcomposite EVA12 with 10 wt.% of fluorohectorite exchanged with ammoniumdodecanoic acid (EVA12–FH/ADA), the nanocomposite of EVA12 with 10 wt.% of montmorillonite exchanged with octadecylammonium (EVA12–MMT/ODA) and the pure EVA12.

of silicate and the type of silicate modification. During thermal degradation, their deacylation is accelerated and may occur at temperatures lower than those for the pure polymer or an EVA–FH/ADA microcomposite due to catalysis by the strongly acid sites created by thermal decomposition of the silicate modifier. These sites are active when there is an intimate contact between the polymer and the silicate. Slowing down of the volatilisation of the deacylated polymer in nitrogen may be due to the labyrinth effect of the silicate layers in the polymer matrix.

In air, the nanocomposite presents a significant delay of weight loss that may derive from the barrier effect due to diffusion of both the volatile thermo-oxidation products to the gas phase and oxygen from the gas phase to the polymer. This barrier effect increases during volatilisation owing to ablative reassembly of the reticular layers of the silicate on the surface of the polymer [12,18].

Acknowledgements

The authors wish to thank Dr Carsten Zilg and Mr Alessandro Riva for their support. The authors also acknowledge support of the Deutsche Forschungsgemeinschaft and Sonderforschungsbereich SFB 428.

References

[1] Katz HS, Milewski JW. Handbook of fillers for plastics. New York: Van Nostrand Reinhold, 1987.
[2] Zanetti M, Lomakin S, Camino G. Macromol Mater Engng 2000;279:1–9.
[3] Giannelis EP. Adv Mater 1996;8:29–35.
[4] Zilg C, Dietsche F, Hoffmann B, Dietrich C, Mülhaupt R. In Proceedings of Eurofiller'99.
[5] Lagaly G, Pinnavaia TJ. Appl Clay Sci 1999:15.
[6] Bridley SW, Brown G, editors. Crystal structure of clay minerals and their X-ray diffraction London: Mineralogical Society, 1980.
[7] Pinnavaia TJ. Science 1983;220:365.
[8] Theng BKG. Formation and properties of clay–polymer complexes. Amsterdam: Elsevier, 1979.
[9] Okada A, Fukoshima Y, Inagaki S, Usuki A, Sugiyama S, Kurashi T, Kamigaito O. US Patent 4,739,007, 1988.
[10] Kurauchi T, Okada A, Nomura T, Nishio T, Saegua S, Deguchi R. SAE Technical Paper Series 910584, 1991.
[11] Gilman JW, Kashivagi T, Nyden M, Brown JET, Jackson CL, Lomakin S, Giannelis EP, Manias E. In: Al-Malaika S, Golovoy A, Wilkie CA, editors. Chemistry and technology of polymer additives. Oxford: Blackwell Science, 1999 (Chap. 14).
[12] Gilman JW, Kashivagi TCL, Giannelis EP, Manias E, Lomakin S, Lichtenhan JD, Jones P. In: Le Bras M, Camino G, Bourbigot S, Delobel R, editors. Fire retardancy of polymer. Cambridge: The Royal Society of Chemistry, 1998.
[13] Zilg C, Reichert P, Dietsche F, Engelhardt T, Mülhaupt R. Kunstoffe 1998;88:1812–20.
[14] Zilg C, Mülhaupt R, Finter J. Macromol Chem Phys 1999;200:661–70.
[15] March J. Advanced organic chemistry. Tokyo: McGraw-Hill Kogakusa, 1977.
[16] Mc Neill. Comprehensive polymer science, vol. 6. Oxford: Pergamon Press, 1989.
[17] Camino G, Sgobbi R, Zaopo, Colombier S, Scelza C. Fire Mater 2000;24:85–90.
[18] Zanetti M, Camino G, Reichert P, Mülhaupt R. Macromol Rapid Comm, in press.